EDINBURGH INSTRUMENTS

50 YEARS 1971-2021

PRECISION RAMAN

Best-in-class Raman microscopes for research and analytical requirements backed with world-class customer support and service.

edinst.com

Received: 15 January 2021 | Revised: 23 April 2021 | Accepted: 25 May 2021

DOI: 10.1002/jrs.6171

SPECIAL ISSUE - RESEARCH ARTICLE

Journal of RAMAN SPECTROSCOPY WILEY

Ultra-compact tunable fiber laser for coherent anti-Stokes Raman imaging

Thomas Gottschall[1] | **Tobias Meyer-Zedler**[2,3] | **Michael Schmitt**[2] | **Robert Huber**[4] | **Juergen Popp**[2,3] | **Andreas Tünnermann**[1,5] | **Jens Limpert**[1,5]

[1]Institute of Applied Physics, Abbe Center of Photonics, Friedrich-Schiller-Universität Jena, Jena, Germany

[2]Institute of Physical Chemistry, Abbe Center of Photonics, Friedrich-Schiller-Universität Jena, Jena, Germany

[3]Leibniz Institute of Photonic Technology, Member of Leibniz Health Technologies, Jena, Germany

[4]Institut für Biomedizinische Optik, Universität zu Lübeck, Lübeck, Germany

[5]Fraunhofer Institute for Applied Optics and Precision Engineering, Jena, Germany

Correspondence
Thomas Gottschall, Institute of Applied Physics, Abbe Center of Photonics, Friedrich-Schiller-Universität Jena, Albert-Einstein-Str. 6, 07745 Jena, Germany.
Email: thomas.gottschall@uni-jena.de

Tobias Meyer-Zedler, Institute of Physical Chemistry, Abbe Center of Photonics, Friedrich-Schiller-Universität Jena, Albert-Einstein-Str. 6, 07745 Jena, Germany.
Email: tobias.meyer@leibniz-ipht.de

Funding information
European Union and the Free state of Thuringia, Grant/Award Number: FKZ IZN 2018 0002; Leibniz Association, Leibniz Science Campus InfectoOptics Jena; German Research Foundation, Grant/Award Number: FKZ EXC 2051/1

Abstract

This work describes the construction of an ultra-compact narrowband fiber laser source for coherent anti-Stokes Raman scattering microscopy of Raman tags, that is, for addressing Raman resonances of deuterated molecules and alkyne tags in the spectral range from 2080 to 2220 cm^{-1}. A narrowband and fast electronically tunable cw seed source based on a semiconductor optical amplifier (SOA) emitting around 1335 nm has been employed to seed four-wave mixing (FWM) in an endlessly single mode fiber (ESM) pumped by a ps pulse duration Yb-fiber laser. A conversion efficiency of 50% is demonstrated. This compact fiber optical parametric amplifier (FOPA) has been used to perform coherent anti-Stokes Raman imaging experiments of crystalline deuterated palmitic acid.

KEYWORDS

coherent anti-Stokes Raman scattering microscopy, four-wave mixing, nonlinear microscopy, ultrafast laser

1 | INTRODUCTION

Coherent Raman scattering microscopies, that is, coherent anti-Stokes Raman scattering (CARS), Raman induced Kerr effect and stimulated Raman scattering microscopy, are extremely powerful and promising methods under investigation for visualization the chemical composition of complex specimen based on the selective excitation of molecular vibrations.[1–3] As a nonlinear imaging method, CRS provides 3D resolved imaging free of out of focus signals, and enables fast imaging in real time for high signal yields. In contrast to spontaneous Raman scattering, however, single wavelength excitation is not sufficient to measure the complete vibrational spectrum covering 0–4000 cm^{-1}. Instead, the specimen interacts with two synchronized ultrashort laser pulses of ps pulse duration, the pump at shorter wavelength and the Stokes at longer wavelength. The molecules are forced to vibrate in phase by illumination with two synchronized pulse trains of a wavenumber difference equal to the wavenumber of a molecular vibration. When pump photons scatter inelastically, the CARS signal is generated, which is blue shifted with respect to the excitation lasers. To probe the full Raman spectrum or a significant fraction thereof, two methods are used: broadband CARS imaging using spectrally broad pulses for excitation which cover a significant part of the Raman spectrum[4–6] or spectral scanning of the wavenumber difference of pump and Stokes laser for time sequential scanning of the Raman spectrum. After the first demonstration of single pulse CARS,[7] further developments in broadband CARS include heterodyne detection,[8] pulse shaping,[9–12] spectral broadening in photonic crystal fibers[10,13,14] and polarization control.[12] The alternative of hyperspectral CARS, that is, time sequential scanning of the frequency difference, is already commercially available.[15–17] So-called hyperspectral CARS microscopy enables efficient signal detection even in turbid media, because also nonballistic photons can be collected by large area single element detectors.[18] For real-time detection of spectral changes, extremely fast tunable laser sources are required. The work presented here aims at the presentation of a compact fiber laser source for the before mentioned approach of hyperspectral CARS microscopy utilizing fast spectrally tuneable narrow band lasers.[19–22] Here, waveguide-based light conversion techniques have become a popular method to convert light to wavelength ranges in which active laser materials do not provide sufficient gain. One concept meeting all demands on a laser source for routine application in medicine and biomedical research is a compact air cooled Yb-fiber laser pump source in combination with four-wave mixing (FWM) in a endlessly single mode fiber (ESM).[23–25] In the simplest realization, FWM starts from quantum noise, such that the spectral width of signal and idler are determined by the phase matching condition of the fiber. For spectrally narrow FWM generation, spectral narrowing of the FWM process can be realized by self-seeding the FWM process with a fraction of the FWM signal or idler wavelength in a fiber optical parametric oscillator (FOPO).[26,27] This results in very compact laser sources providing tunable emission across the range of optical parametric generation within the fiber defined by the specific pump wavelength and the phase matching condition of the fiber. Alternatively, the FWM process can be seeded using an external laser source of narrow emission, for example, a cw Ti:Sapphire laser operating in the signal wavelength range of the FWM process.[28] While very little seed power is needed, that is, on the order of 5 mW cw seed, the whole laser source is large due to the large seed laser and the seed power is also adding to the photon load on the specimen when using the Ti:Sapphire seeded FWM pump as the CARS pump wavelength. In recent years, imaging of Raman labels in the wavenumber range around 2000 cm^{-1} has become an area of intense research,[29,30] that is, for imaging the glucose metabolism[31] or the protein metabolism.[32] This method enables to investigate smaller biomolecules than possible with fluorescence at low concentration and with high contrast, since the spectral range around 2000 cm^{-1} is apart from C-C- or C-N-triple bonds and carbon–deuterium-stretch vibrations devoid of vibrations. In addition, triple bond Raman signals are very intense as are Raman signals from carbon-deuterium stretch vibrations of fully deuterated molecules. For widespread application of this technique in life sciences, robust and easy to use laser sources for CARS microscopy working in this spectral range are highly desired.

In this contribution, a novel Yb-fiber laser source for CARS microscopy in the wavenumber range from 2000 to 2320 cm^{-1} for imaging Raman tags like alkynes and carbon-deuterium functional groups is presented. For seeding of the FWM process in an ESM fiber at the idler wavelength, a semiconductor optical amplifier (SOA) working at about 1335 nm has been employed. The SOA enables fast tuning from 1315–1370 nm, such that th wavenumber difference of FWM signal and Yb-fundamental addresses Raman resonances around 2100 cm^{-1}. This laser concept has been applied to CARS imaging of a crystal of fully deuterated palmitic acid at 2100 cm^{-1} with high contrast.

2 | RESULTS AND DISCUSSION

The laser setup specifically designed for CARS microscopy in the spectral range of Raman tags around

2100 cm^{-1} is depicted in Figure 1. The pump pulses used for the optical parametric amplifier are generated in a passively mode-locked Yb-fiber laser operating at a repetition rate of 20.55 MHz. The fiber laser of fs pulse duration uses a narrowband fiber Bragg grating with a bandwidth of 0.04 nm as outcoupling mirror to directly produce narrowband pulses centered at 1040.4 nm with a pulse duration of 120 ps. To increase the peak power of the pump pulses without the need for excessive amount of pump power, the repetition rate is divided by a synchronous down counter by 25 to 822 kHz. The reduction of the pulse repetition rate is accomplished by a fiber coupled acousto-optical modulator. Since for pulses in the picosecond range the nonlinearity of optical damage of tissue is lower than the order of nonlinearity of the CARS process, this reduced repetition rate is advantageous and maximizes the signal.[33,34] As a consequence, the repetition rate of the CARS pump and Stokes pulses should be low enabling using intense pulses of kW peak power at moderate average power levels, which justifies the low repetition rate in the experiments performed here.[22] The repetition rate is also adjusted to fit the lowest pixel dwell time of 1 µs used in the imaging experiments, which is also determined by the bandwidth of the custom-built preamplifier of 500 kHz (Pascher instruments AB, Lund, Sweden). The laser pulses at the reduced repetition rate are subsequently amplified in a two-stage amplifier, which boosts the average power up to 400 mW.

The amplified laser pulses are then coupled into an ESM fiber of 55 cm length, single missing hole design, hole to hole distance 3.2 µm and hole diameter 1.4 µm (NKT-Photonics, Birkerød, Denmark), which provides the parametric gain at around 850 and 1330 nm via FWM when pumped at 1040.4 nm.[23]

For seeding the FWM process and spectral tuning, a tunable continuous wave (cw) oscillator is combined with the amplified Yb-laser emission using a longpass dichroic mirror before coupling cw seed and Yb-pulses into the ESM fiber. The tunable cw oscillator consists of a semiconductor optical amplifier (Thorlabs BOA 1130S) and a tunable Fabry-Pérot filter (Lambda Quest). The directionality is ensured by two isolators. The cavity uses a tap coupler to extract about 70% of the circulating power per

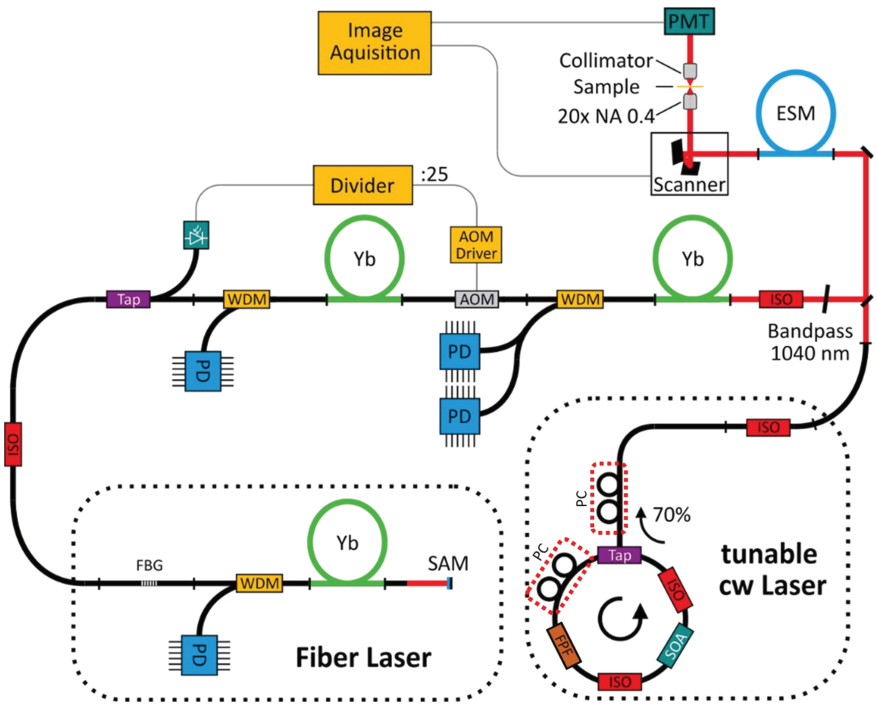

FIGURE 1 Setup of the cw seeded FOPA. The tunable cw laser has a ring cavity including a tunable Fabry-Pérot filter (FPF), a semiconductor optical amplifier (SOA), isolators (ISO), a 30:70 tap coupler, and a polarization controller (PC). The fiber laser consists of an ytterbium-doped single fiber (Yb), a wavelength division multiplexer (WDM), a pump diode (PD) emitting at 976 nm, a fiber Bragg grating (FBG), and a saturable absorber mirror (SAM). The fiber laser is sampled with a 5% tap coupler (Tap) and amplified in two stages with an acousto-optical modulator (AOM) in between to reduce the repetition rate. Both outputs are overlapped and coupled to an endlessly single mode (ESM, 55 cm long, single missing hole design, hole to hole distance 3.2 µm, and hole diameter 1.4 µm) fiber. The output is coupled to a laser scanning microscope equipped with a NA 0.4 NIR objective and a photo-multiplier tube (PMT) for detection

round trip. Polarization controllers are used to maximize the circulating power and to adjust the polarization of the SOA to the polarization of the Yb-pump light in the ESM fiber. After adjusting the central wavelength to the gain bandwidth range of the FWM process, that is, ~1330 nm, the light seeds the process which dramatically decreases the bandwidth of the generated signal and idler light.[28] Since the seeding light is continuous, complex synchronization and stabilization electronics are not required.

The conversion efficiency is highly dependent on the pump power, which drives the nonlinear conversion process (Figure 2). As the Yb-pump pulses experiences self-phase modulation (SPM) during conversion, also the spectral bandwidth of the signal and idler pulses increases from 0.25 nm at 67 mW to 0.75 nm at 200 mW (Figure 2). Apart from SPM induced broadening of the Yb-pump pulses, pump depletion and self-phase modulation of the converted signal itself also contribute to the observed broadening of the signal with increasing pump power. Still, 0.75 nm bandwidth correspond to 10 cm^{-1} only, which is still significantly smaller than the bandwidth of the parametric gain without seed. At 785 nm, >50 cm^{-1} bandwidth have been obtained at a comparable signal power of 72 mW.[24] The dependence of bandwidth and average pump power of the signal and idler pulses for the presented laser are depicted in Figure 2b. It is evident, that while for higher peak powers the signal bandwidth increases, the bandwidth at maximum pump power of 200 mW of 10 cm^{-1} is still as low as a transform limited 2 ps Gaussian pulse, which is the state-of-the-art laser source for CARS microscopy today. A further increase of the pump power leads to an onset of super continuum generation and the peak power of the process is reaching a maximum.[28]

Another advantage of the presented FOPA laser is the high conversion efficiency. In the presented experiment it was possible to convert more than 50% of the pump power to the signal and idler at pump powers exceeding 200 mW, which is significantly better than the conversion efficiencies for self-seeded FWM in FOPOs. Here, 20% up to 38% conversion efficiency have been achieved.[26,35] The average power corresponds to a peak power of 2 kW when assuming, that the signal pulse has the same pulse duration as the Yb-pump of 120 ps. The nonlinear phase $B = \gamma Pl$, which governs the process is 11 rad in this case. The resulting signal spectra at different pump powers are plotted in Figure 2a.

The spectral width of the signal wavelength at an average pump power of 150 mW is 0.59 nm due to SPM and the filter bandwidth of the tunable Fabry-Pérot filter (FPF). This bandwidth corresponds to a spectral resolution of 8 cm^{-1}, which is a factor of 10 higher compared to seeding with a spectrally narrow Ti:Sapphire laser.[28] For the imaging experiments the pump power has been fixed to this value to limit the risk of photo induced damage, since the converted power of 50 mW signal and idler is sufficient for all CARS microscopy experiments.

For spectral tuning, different seed wavelengths are generated by applying different voltages to the tunable Fabry-Pérot filter (FPF). Similar filters elements enable spectral tuning up to MHz sweep rates in Fourier domain mode-locked lasers used for OCT imaging.[36–38] A very similar FPF has been used before in an Fourier domain mode-locked laser.[36] In this case the maximum achievable tuning speed has been limited by the optical round trip time in the cavity enabling sweep repetition rates of more than 10 kHz. In case of operating the laser source in a wavelength agile tuning mode rather than a continuous sweep mode, meaning in a mode where arbitrary jumps

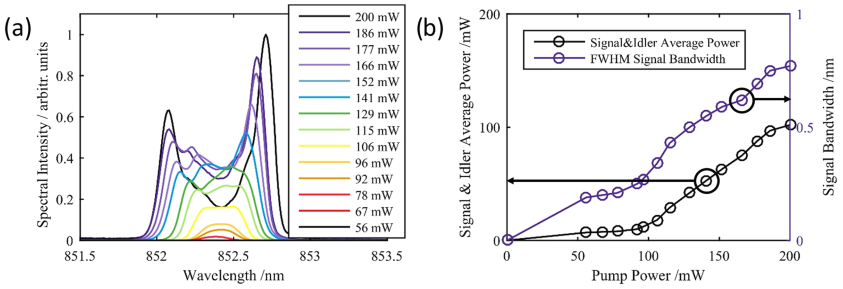

FIGURE 2 (a) Spectral signal evolution for pump power in the range of 56 and 200 mW for pumping at 1040.4 nm and seeding at 1335 nm, which is at the FWM gain maximum for this pump wavelength (see Figure 3a). The spectral broadening of the signal with increasing pump power at 1040.4 nm results from self-phase modulation. (b) The extracted signal and idler average power at the FWM gain maximum for pumping at 1040.4 nm after the parametric amplification (black trace and black dots) increases with the pump power at 1040.4 nm. At 200 mW pump power, the power of signal and idler is 100 mW, which corresponds to a FWM conversion efficiency of 50%. The FWHM spectral bandwidth of the signal is increasing due to self-phase modulation from 0.25 nm at 50 mW pump power up to 0.75 nm at 200 mW pump power (blue trace)

between wavelengths should be performed, around 100 μs step response time can be realized for large wavelength steps. The cw oscillator enables generating seed wavelengths between 1312 and 1371 nm by tuning the FPF. This results in signal wavelengths between 838 and 861 nm (Figure 3b). Significant conversion occurs between 845 and 855 nm for the signal, that is, between 1353 and 1328 nm for the cw seed and idler, addressing Raman resonances from 2220 to 2085 cm^{-1}, which corresponds to the maximum parametric gain of the ESM when pumped at 1040.4 nm. The cw seed average power coupled to the ESM conversion fiber was approximately 10 mW during the experiments. The resulting average power of both the signal and idler average power is plotted in Figure 3a. Note that also the cw seed power is included in the power of the idler plotted in Figure 3a. In the spectral range from 845 to 855 nm a signal average power of 10 to 30 mW could be generated at 150 mW pump power and fixed pump wavelength of 1040.4 nm (Figure 3a). Considering the repetition rate of the pump laser of 822 kHz and the signal pulse duration of 65 ps measured with a 30 GHz real-time oscilloscope and a photo diode with 18 ps rise time, the average power corresponds to a signal peak power of 190 to 560 W.

As can be seen in Figure 3a, the signal power conversion distribution around the maximum conversion wavelength is asymmetric decaying faster at lower wavenumber differences with respect to the pump. This asymmetric shape of the signal power around the central gain bandwidth can be explained by the phase matching of the FWM process, which is not only dependent on the nonlinear phase of the pump peak power but also by that of the signal and idler. Consequently, as the conversion efficiency increases, the gain maximum shifts towards the pump wavelength.

The residual pump pulse bandwidth at 150 mW pump power has been determined to be 0.36 nm, which corresponds to 3.3 cm^{-1} FWHM. The signal bandwidth for these parameters is 0.59 nm corresponding to 8.1 cm^{-1} (Figure 2b). Hence, the resulting spectral resolution for the CARS experiments is ~10 cm^{-1}. Of course, as the signal power decreases towards the edges of the tunable bandwidth, the signal bandwidth decreases also, since there is no significant SPM at low power. Still, the spectral resolution of 10 cm^{-1} is comparable to the spectral width of a standard OPO laser source of 2 ps pulse duration and transform limited pulses.

To prove the suitability of the presented laser source for CARS microscopy, imaging experiments have been performed. The laser source is coupled into a laser scanning microscope, which has been previously described in detail.[39] In brief, the laser of 20 mW pump power at 853 nm and 90 mW Stokes laser power at 1040.4 nm is coupled into a custom laser scanning microscope (LSM, Pascher Instruments AB, Lund, Sweden) and focused onto the specimen by a 20x NA 0.4 apochromatic objective (NIR APO, Mitutoyo, Japan). For CARS imaging, a crystal of deuterated palmitic acid (palmitic acid-d31, CAS 39756–30-4, Merck) has been investigated in resonance with the symmetric C-D-stretch vibration of fully deuterated methylene groups at 2100 cm^{-1} (pump 853.88 nm) and off resonance at 2135 cm^{-1} (pump 851.4 nm). The CARS signal is collected in forward direction by an aspheric condenser lens of 25 mm diameter and 20 mm focal length (Asphericon, Jena, Germany), filtered from the excitation laser light by two short pass filters at 770 nm (FF01-770/SP-25, Semrock, USA) and 750 nm (FESH0750, Thorlabs, USA) and a band pass filter centered at 720 nm (FF01-720/24-25, Semrock, USA) and detected by a

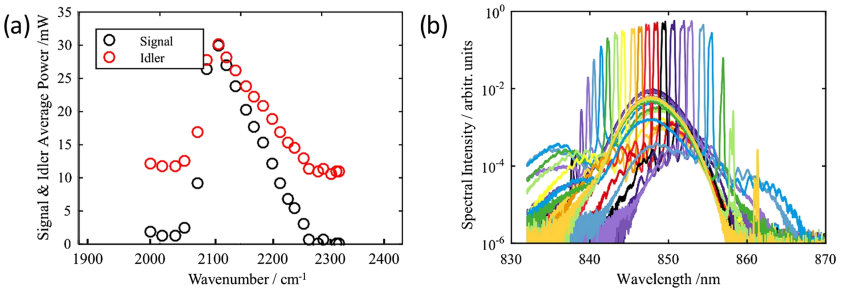

FIGURE 3 (a) Average power of FWM signal (black dots) and idler (red dots) plotted as a function of wavenumber, that is, the difference of signal wavenumber and Yb-wavenumber or the difference of Yb-wavenumber and idler wavenumber, at constant pump power of 150 mW at 1040.4 nm. The plotted idler power is including the cw seed of ~10 mW average power. Hence, the idler power of ~10 mW at close to zero signal power corresponds to the cw seed power, when there is no significant conversion efficiency. (b) Signal spectra for the measurement points plotted in panel (a). For clarity each measurement is individually colored. At the spectral edges of the working range of FWM when pumped at 1040.4 nm, the FWM conversion efficiency is almost 4 orders of magnitude lower compared to the wavelength of maximum FWM conversion around 850 nm

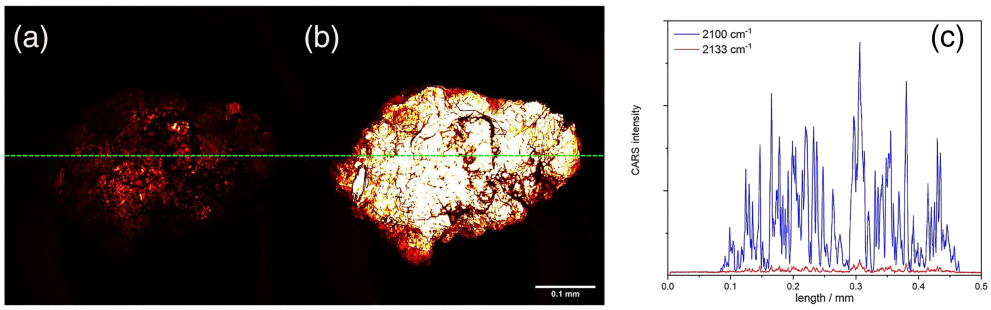

FIGURE 4 CARS microscopic imaging experiments of a crystal of deuterated palmitic acid using 20 mW pump, 90 mW Stokes power. Image parameters: Field of view 500 µm, 2048 pixels, 16 bit image depth, 480 mV PMT control voltage. (a) CARS image of a crystal of palmitic acid-d31 off resonant at 2135 cm^{-1}. (b) Resonant CARS microscopic image a crystal of palmitic acid-d31 at 2100 cm^{-1}. Along the green dashed line indicated in images (a) and (b) CARS intensity line profiles are plotted in panel (c). The ratio of resonant to nonresonant signal is about 22:1

photo-multiplier tube (PMT, H10721-20, Hamamatsu, Japan). The resulting images are depicted in Figure 4 together with intensity profiles along the indicated line. The image contrast is 22:1, proving high contrast chemical imaging with this laser source. In the spectral range around 2100 cm^{-1}, Raman resonances are rare in biological specimen, which is why this spectral range is used for vibrational labeling. Seeded FWM-based laser sources have been realized in the CH-stretching spectral range proving high contrast CARS imaging of biological specimen.[28,40] In addition, the PMT control voltage of 480 mV is only 50% of the maximum control voltage, such that also much lower CARS signals can be measured.

3 | CONCLUSION

In this work a compact and tunable fiber laser source for CARS microscopy in the spectral range of Raman tags has been presented and application to imaging a crystal of deuterated palmitic acid has been demonstrated. The fiber laser concept allows for 10 nm fully electronic tuning centered at 850 nm, that is, from 2220 to 2085 cm^{-1}, at a sweep rate equivalent to the laser repetition rate of 822 kHz and can be realized all-fiber without free space optics or moving parts, enabling routine application outside specialized laser labs. The spectral resolution of 10 cm^{-1} compares well with current state-of-the-art bulk OPO laser sources of 2 ps pulse duration and 80 MHz repetition rate. Higher spectral resolution is possible, as has been previously demonstrated for a FOPA[28] but also for a FOPO.[26] At the same average power of 30 mW at the sample site, the peak power of up to 560 W is three times larger than the peak power of a 80 MHz laser of 2 ps pulse duration. In case of two photon excited fluorescence it has been shown, that longer pulse durations are beneficial for reducing nonlinear photodamage.[41,42] The long pulse duration also relaxes the problem of temporal synchronization of the pump and Stokes laser pulses enabling endoscopic applications and flexible fiber delivery of the lasers.[43–45] The long pulse duration results also in narrow spectral widths, which is also reducing temporal broadening by group velocity dispersion. If higher average powers are needed, power scaling by increasing the repetition rate is possible. An increase by a factor of 10 can be realized. For applications requiring high repetition rates like fluorescence lifetime imaging and fast imaging using pixel dwell times below 1 µs, a laser of low repetition rate and long pulse duration performs worse compared to a high repetition rate laser source. Furthermore, the FOPA provides conversion efficiencies up to 50%. For the FOPO, 38% conversion efficiency has been demonstrated.[26] Another advantage of the FOPA concept is the fast spectral tuning speed. When the seed is present, narrowband FWM signal and idler emission is generated in presence of the pump pulse. Hence, the FOPA tuning speed is limited by the spectral tuning of the seed laser source only, such that pulse-to-pulse spectral tuning can be achieved, which is the fastest possible tuning speed. In conclusion, while an SOA based laser source has been previously realized,[46] in the presented work such a laser is to the best of our knowledge for the first time successfully applied to CARS microscopy paving the way towards application of CARS and other coherent Raman imaging methods in routine diagnostics and biomedical research.

ACKNOWLEDGMENTS

We thank Active Fiber Systems GmbH for the control hardware of the fiber oscillator and amplifier unit. TMZ,

MS, and JP gratefully acknowledge financial support from the German Research Foundation (DFG) via the Cluster of Excellence Balance of the Microverse (FKZ EXC 2051/1), by the Leibniz Science Campus InfectoOptics Jena (projects FastDrop, VesaDrop, iTag), which is financed by the funding line Strategic Networking of the Leibniz Association and by the European Union and the Free state of Thuringia via the Thüringer Innovationszentrum für Medizintechnik-Lösungen (ThIMEDOP) (FKZ IZN 2018 0002).

ORCID

Thomas Gottschall https://orcid.org/0000-0001-9369-4205
Tobias Meyer-Zedler https://orcid.org/0000-0001-6740-629X
Michael Schmitt https://orcid.org/0000-0002-3807-3630
Robert Huber https://orcid.org/0000-0001-9785-6574
Juergen Popp https://orcid.org/0000-0003-4257-593X
Jens Limpert https://orcid.org/0000-0001-8349-3530

REFERENCES

[1] A. Zumbusch, G. R. Holtom, X. S. Xie, *Phys. Rev. Lett.* **1999**, *82*, 4142.
[2] C. W. Freudiger, M. B. J. Roeffaers, X. Zhang, B. G. Saar, W. Min, X. S. Xie, *The Journal of Physical Chemistry B* **2011**, *115*, 5574.
[3] C. W. Freudiger, W. Min, B. G. Saar, S. Lu, G. R. Holtom, C. He, J. C. Tsai, J. X. Kang, X. S. Xie, *Science* **2008**, *322*, 1857.
[4] N. Dudovich, D. Oron, Y. Silberberg, *J Chem Phy* **2003**, *118*, 9208.
[5] C. H. Camp Jr., M. T. Cicerone, *Nat. Photonics* **2015**, *9*, 295.
[6] C. H. Camp Jr., Y. J. Lee, J. M. Heddleston, C. M. Hartshorn, A. R. H. Walker, J. N. Rich, J. D. Lathia, M. T. Cicerone, *Nat. Photonics* **2014**, *8*, 627.
[7] N. Dudovich, D. Oron, Y. Silberberg, *Nature* **2002**, *418*, 512.
[8] B. von Vacano, T. Buckup, M. Motzkus, *Opt. Lett.* **2006**, *31*, 2495.
[9] B. von Vacano, M. Motzkus, *Opt. Commun.* **2006**, *264*, 488.
[10] B. von Vacano, W. Wohlleben, M. Motzkus, *Opt. Lett.* **2006**, *31*, 413.
[11] B. von Vacano, W. Wohlleben, M. Motzkus, *J. Raman Spectrosc* **2006**, *37*, 404.
[12] B. von Vacano, M. Motzkus, *Phys. Chem. Chem. Phys.* **2008**, *10*, 681.
[13] B. von Vacano, L. Meyer, M. Motzkus, *J. Raman Spectrosc* **2007**, *38*, 916.
[14] J. Rehbinder, C. Pohling, T. Buckup, M. Motzkus, *Opt. Lett.* **2010**, *35*, 3721.
[15] R. S. Lim, J. L. Suhalim, S. Miyazaki-Anzai, M. Miyazaki, M. Levi, E. O. Potma, B. J. Tromberg, J. Lipid, *Res.* **2011**, *52*, 2177.
[16] C.-Y. Lin, E. Potma, J. Suhalim, C. L. Nien, J. Jester, M. Miljkovic, M. Diem, *J. Biomed. Opt.* **2011**, *16*, 021104.
[17] M. Ji, M. Arbel, L. Zhang, C. W. Freudiger, S. S. Hou, D. Lin, X. Yang, B. J. Bacskai, X. S. Xie, *Sci. Adv.* **2018**, *4*, eaat7715.
[18] R. Arora, G. Petrov, V. Yakovlev, *J. Biomed. Opt.* **2011**, *16*, 021116.
[19] R. Selm, M. Winterhalder, A. Zumbusch, G. Krauss, T. Hanke, A. Sell, A. Leitenstorfer, *Opt. Lett.* **2010**, *35*, 3282.
[20] A. F. Pegoraro, A. Ridsdale, D. J. Moffatt, J. P. Pezacki, B. K. Thomas, L. Fu, L. Dong, M. E. Fermann, A. Stolow, *Opt. Express* **2009**, *17*, 20700.
[21] K. Kieu, B. G. Saar, G. R. Holtom, X. S. Xie, F. W. Wise, *Opt. Lett.* **2009**, *34*, 2051.
[22] T. Gottschall, T. Meyer, M. Baumgartl, C. Jauregui, M. Schmitt, J. Popp, J. Limpert, A. Tunnermann, *Laser Photonics Rev.* **2015**, *9*, 435.
[23] M. Baumgart, T. Gottschall, J. Abreu-Afonso, A. Diez, T. Meyer, B. Dietzek, M. Rothhardt, J. Popp, J. Limpert, A. Tunnermann, *Opt. Express* **2012**, *20*, 21010.
[24] M. Baumgartl, M. Chemnitz, C. Jauregui, T. Meyer, B. Dietzek, J. Popp, J. Limpert, A. Tunnermann, *Opt. Express* **2012**, *20*, 4484.
[25] K. W. Yang, Y. X. Wu, J. S. Jiang, P. B. Ye, K. Huang, Q. Hao, H. P. Zeng, *Ieee Photonics Technology Letters* **2018**, *30*, 967.
[26] T. Gottschall, T. Meyer, M. Baumgartl, B. Dietzek, J. Popp, J. Limpert, A. Tunnermann, *Opt. Express* **2014**, *22*, 21921.
[27] T. Gottschall, T. Meyer, M. Schmitt, J. Popp, J. Limpert, A. Tunnermann, *Opt. Express* **2015**, *23*, 23968.
[28] M. Chemnitz, M. Baumgartl, T. Meyer, C. Jauregui, B. Dietzek, J. Popp, J. Limpert, A. Tunnermann, *Opt. Express* **2012**, *20*, 26583.
[29] L. Wei, F. Hu, Z. Chen, Y. Shen, L. Zhang, W. Min, *Acc. Chem. Res.* **2016**, *49*, 1494.
[30] Z. Zhao, Y. Shen, F. Hu, W. Min, *Analyst* **2017**, *142*, 4018.
[31] R. Long, L. Zhang, L. Shi, Y. Shen, F. Hu, C. Zeng, W. Min, *Chem. Commun.* **2018**, *54*, 152.
[32] L. Wei, Y. Shen, F. Xu, F. Hu, J. K. Harrington, K. L. Targoff, W. Min, *ACS Chem. Biol.* **2015**, *10*, 901.
[33] K. König, H. Liang, M. W. Berns, B. J. Tromberg, *Nature* **1995**, *377*, 20.
[34] K. König, T. W. Becker, P. Fischer, I. Riemann, K. J. Halbhuber, *Opt. Lett.* **1999**, *24*, 113.
[35] E. S. Lamb, S. Lefrancois, M. Ji, W. J. Wadsworth, X. Sunney Xie, F. W. Wise, *Opt. Lett.* **2013**, *38*, 4154.
[36] R. Huber, M. Wojtkowski, K. Taira, J. G. Fujimoto, K. Hsu, *Opt. Express* **2005**, *13*, 3513.
[37] R. Huber, M. Wojtkowski, J. G. Fujimoto, *Opt. Express* **2006**, *14*, 3225.
[38] S. Karpf, M. Eibl, W. Wieser, T. Klein, R. Huber, *Nat. Commun.* **2015**, *6*, 6784.
[39] T. Meyer, M. Baumgartl, T. Gottschall, T. Pascher, A. Wuttig, C. Matthaeus, B. F. M. Romeike, B. R. Brehm, J. Limpert, A. Tuennermann, O. Guntinas-Lichius, B. Dietzek, M. Schmitti, J. Popp, *Analyst* **2013**, *138*, 4048.
[40] T. Meyer, M. Chemnitz, M. Baumgartl, T. Gottschall, T. Pascher, C. Matthaus, B. F. M. Romeike, B. R. Brehm, J. Limpert, A. Tunnermann, M. Schmitt, B. Dietzek, J. Popp, *Anal. Chem.* **2013**, *85*, 6703.
[41] H. J. Koester, D. Baur, R. Uhl, S. W. Hell, *Biophys. J.* **1999**, *77*, 2226.
[42] A. Hopt, E. Neher, *Biophys. J.* **2001**, *80*, 2029.
[43] P. Zirak, G. Matz, B. Messerschmidt, T. Meyer, M. Schmitt, J. Popp, O. Uckermann, R. Galli, M. Kirsch, M. J. Winterhalder, A. Zumbusch, *APL Photonics* **2018**, *3*, 092409.

[44] A. Lukic, S. Dochow, H. Bae, G. Matz, I. Latka, B. Messerschmidt, M. Schmitt, J. Popp, *Optica* **2017**, *4*, 496.
[45] A. Lombardini, V. Mytskaniuk, S. Sivankutty, E. R. Andresen, X. Q. Chen, J. Wenger, M. Fabert, N. Joly, F. Louradour, A. Kudlinski, H. Rigneault, *Light Sci. Appl.* **2018**, 7.
[46] I. Aporta, M. A. Quintela, J. M. Lopez-Higuera, J. Lightwave, *Technol.* **2019**, *37*, 3510.

How to cite this article: T. Gottschall, T. Meyer-Zedler, M. Schmitt, R. Huber, J. Popp, A. Tünnermann, J. Limpert, *J Raman Spectrosc* **2021**, *52*(9), 1561. https://doi.org/10.1002/jrs.6171